JOURNAL OF FUNDAMENTAL MATHEMATICS
AND APPLICATIONS (JFMA) VOL. 8 NO. 1 (2025)
Available online at www.jfma.math.fsm.undip.ac.id

EPIDEMIC ANALYSIS, MATHEMATICAL MODELLING AND NUMERICAL SIMULATION OF COVID-19 TRANSMISSION

Eka Triyana[1*], Widowati[2]

[1]*Mathematics Education Study Program, Pattimura University, Ambon, Indonesia*
[2]*Department of Mathematics, Universitas Diponegoro, Semarang, Indonesia*

Email: [1] eka.triyana@lecturer.unpatti.ac.id , [2] widowati@lecturer.undip.ac.id
[*]Corresponding

Abstract. This research develops a model with seven compartments SEIQDHR for the spread of COVID-19, with detected and treated individual behavior changes affecting disease transmission. The Next Generation Matrix is used to analyze local and global stability and to calculate the basic reproduction number. Then, the analysis of disease-free equilibrium and endemic equilibrium. Stability analysis shows that the equilibrium point is locally asymptotically stable when the basic reproduction number is less than one and globally asymptotically stable when it is greater than one. The results of the sensitivity analysis show that the transmission rate, the progression rate from exposure, and the detection rate are parameters that significantly influence the dynamics of disease spread. Numerical simulations were used to validate the analysis results and identify key parameters that contribute most to the spread of the disease among affected, infected, quarantined, diagnosed, and hospitalized individuals.

Keywords: epidemiological model; COVID-19; detected or diagnosed, sensitive analysis, stability analysis.

I. INTRODUCTION

In the last decade, a number of new diseases, from the deadly Ebola virus, Zika, HIV, HBV, H1N1 and malaria have tested the global healthcare system and put at-risk populations that have emerged in various parts of the world. This represents a significant challenge to global health security and the need to prepare and implement rapid response strategies. One of the most recent and influential pathogens is the coronavirus, which was first identified in Wuhan, China. The new virus, known as SARS-CoV-2, is a symptom for many people with respiratory diseases [1], [2], [3], [4], [5]. The coronavirus disease 2019 (COVID-19) is now a global pandemic. The coronavirus pandemic, COVID-19, has claimed the lives of thousands of people globally, prompting several regions and governments to close their borders, with global ramifications that remain unknown. Although the human-to-human transmission route for this disease has been proven, the mechanism of transmission remains unexplained. This is a global public health crisis unlike any other in recent memory. [6]. Mathematical models are commonly used in many fields, such as socioeconomic [7], [8], [9], [10], [11], medicine [12], [13], education [14], agriculture[15], [16], environment [17], [18], [19] and references cited therein. Mathematical models have been used in the health sector to prevent, detect, and treat disease

epidemics. One of them is used to study the spread of disease. Researchers have proposed various mathematical models to analyze the spread and perform simulations aimed at prediction [20].

Mata and Dourad, they make a substantial contribution with their study of mathematical modeling used in epidemiology. The model that has been developed is a deterministic SIR model that is computer-simulated [21], [22], [23], [24], [25]. Using a nonlinear mathematical model, the author studies the dynamics of malaria transmission in a population, and the theory of differential equation stability is applied. computing the reproduction number as a stable asymptotic condition for both endemic and disease-free equilibrium [26]. Das et al. [27] their study focusses on The SEIR pandemic tuberculosis transmission model was analyzed using a mathematical model with four compartments. They investigate the effects of various compartment phases by analyzing infections at disease-free equilibrium along with the basic reproduction number, system strength, and at the endemic equilibrium point. This model was tested for local and global asymptotic stability at the disease-free equilibrium point when the basic reproduction number is less than one, as well as the new endemic equilibrium when the basic reproduction number exceeds one. The bifurcation investigation was carried out using bifurcation techniques from central manifold theory.

Jonnalagadda and Mohan [28] proposed a mathematical model to study the dynamics of COVID-19 transmission by considering the Susceptible, Latent, Infected, Recovered, and Vaccinated. Haq et al [29] developed the model SVEIQR comprises the following compartments: susceptible, vaccinated, exposed, infected, quarantine, and recovered. Mishraa et al [30] formulated a mathematical model into six classes, namely susceptible, exposed, infected, asymptomatic, quarantine/isolation, and recovered (SEIQAR). The authors consider the reproduction number, elasticity, and sensitivity analysis showed sensitive to the parameter the Lyapunov function is used to analyse the global stability of the model**.**

The novelty of this paper is found in its thorough investigation of a deterministic mathematical model aimed at understanding the dynamics of COVID-19, by adding the detected and hospitalize compartments. We integrated detected and hospitalised compartment into the $SEIQDHR$ framework in our suggested model. The article is structured in the following manners: Section 2 deals with the development and explanation of the mathematical model. Section 3 considers the solution's existence and uniqueness for the model developed. In section 4, we derive the basic reproduction number evaluate the disease-free equilibrium and its local stability, as well as both the endemic equilibrium's local and global stabilities. Section 5 provides a sensitivity analysis of the parameters of the model in order to find the major determinants of the disease dynamics. In section 6, simulations are done using MATLAB, we validate the model and also showcase the qualitative findings of the model. Finally, section 7 is for the conclusion of the paper where a brief recap is presented

II. FORMULATION OF THE MODEL

The spread of infectious diseases can occur in a complex manner due to the interaction between various variables. One of the methods used to analyze and project the patterns of spread and severity of the disease is through mathematical models. We considering the SEIQDHR model subdivides the human population into six compartments; Susceptible (S), Exposed (E), Infected (I) , Quarantined (Q), Detected or diagnosed (D), Hospitalize (H), and Recovered (R). Based on this consideration, the total population is $N(t) = S(t) + E(t) + I(t) + Q(t) + D(t) + H(t) + R(t)$. The mathematical model that describes Covid transmission dynamics is illustrated in Fig. 1. All paremeters are explained in Table 1.

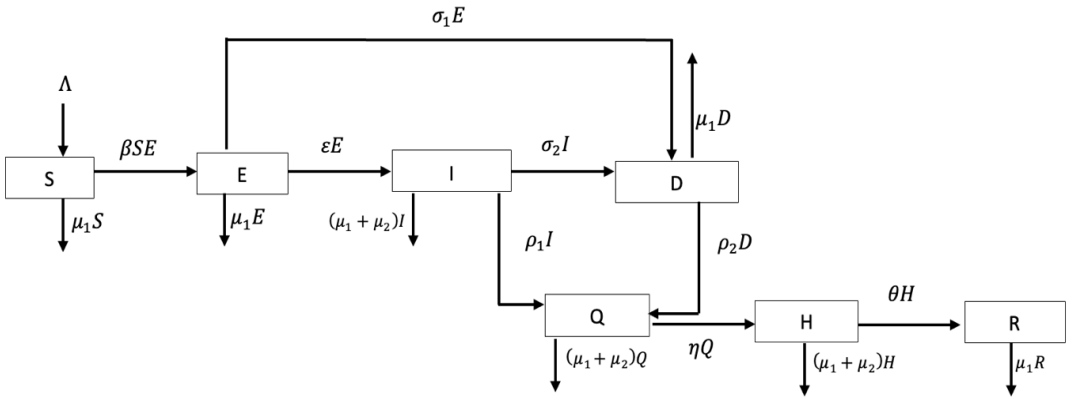

Figure 1. Flow diagram of the formulated model

Table 1. Parameters

Parameters	Description
Λ	Natural natality rate of susceptible individuals
β	The transmission rate of exposed getting infectious
μ_1	Natural mortality rate
μ_2	the death rate due to COVID-19
ε	Progression rate from exposed individuals to infectious individual
σ_1	Rate for the detection of exposed individual
σ_2	Rate for the detection of infected individual
ρ_1	Quarantine rate of individuals from infected individuals
ρ_2	Quarantine rate following Diagnosed
η	Recovery rate for individuals in quarantined
θ	Recovery rate of hospitalized population

Through the schematic diagram depicted in Figure 1, a system of nonlinear differential equations is obtained and presented below:

$$\begin{aligned}
\frac{dS}{dt} &= \Lambda - \beta SE - \mu_1 S \\
\frac{dE}{dt} &= \beta SE - \varepsilon E - \sigma_1 E - \mu_1 E \\
\frac{dI}{dt} &= \varepsilon E - \sigma_2 I - \rho_1 I - (\mu_1 + \mu_2) I \\
\frac{dD}{dt} &= \sigma_1 E + \sigma_2 I - \rho_2 D - \mu_1 D \\
\frac{dQ}{dt} &= \rho_1 I + \rho_2 D - \eta Q - (\mu_1 + \mu_2) Q \\
\frac{dH}{dt} &= \eta Q - \theta H - (\mu_1 + \mu_2) H \\
\frac{dR}{dt} &= \theta H - \mu_1 R.
\end{aligned} \tag{1}$$

Initial values are $S(0) \geq 0, E(0) \geq 0, I(0) \geq 0, D(0) \geq 0, Q(0) \geq 0, H(0) \geq 0, R(0) \geq 0$.

From the sum of all differential equations in system (1) is

$$\frac{dN}{dT} = \Lambda - \mu_1 N - \mu_2(I + Q + H). \tag{2}$$

III. BASIC QUALITATIVE ANALYSIS

Since the model represents a human population which cannot be negative, we need to ensure that all state variables remain non-negative with the initial value condition of system (1) are positive in the bounded region, so that this model is epidemiologically relevant.

3.1 Non-negativity and Boundedness of the solutions

We first present the nonnegativity theorem as follows:

Theorem 1. *(Non-negativity of the solutions): Given non-negative initial condition* $S(0) \geq 0, E(0) \geq 0, I(0) \geq 0, D(0) \geq 0, Q(0) \geq 0, H(0) \geq 0,$ *and* $R(0) \geq 0$*the solutions of set* $\{S(t), E(t), I(t), D(t), Q(t), H(t), R(t)\}$ *of the system (1) are non-negative for all* $t \geq 0$.

Proof. From the second equation of system (1) we have that

$$\frac{dE}{dt} = \beta SE - \varepsilon E - \sigma_1 E - \mu_1 E$$

$$\frac{dE(t)}{dt(t)} + (-\beta S(t) + \varepsilon + \sigma_1 + \mu_1\,)E(t) \geq 0. \tag{3}$$

Multiplying the inequality (3) by $exp\left(\int_0^t (-\beta S(u) + \varepsilon + \sigma_1 + \mu_1\,)du\right)$ we have

$$\frac{dE(t)}{dt(t)} \cdot exp\left(\int_0^t (-\beta S(t) + \varepsilon + \sigma_1 + \mu_1\,)d\,t\right) + (-\beta S(t) + \varepsilon + \sigma_1 + \mu_1\,)E(t)$$

$$\cdot exp\left(\int_0^t (-\beta S(t) + \varepsilon + \sigma_1 + \mu_1\,)dt\right) \geq 0.$$

Then

$$\frac{d}{dt(t)}\left(E(t) \cdot exp\left(\int_0^t (-\beta S(u) + \varepsilon + \sigma_1 + \mu_1\,)du\right)\right) \geq 0, \forall t \geq 0,$$

and thus

$$E(t) \geq E(0) \cdot exp\left(-\int_0^t (-\beta S(u) + \varepsilon + \sigma_1 + \mu_1\,)d\,u\right).$$

Therefore, the solution $E(t)$ is positive. In the same way, we are proving that

$S(t) \geq 0, E(t) \geq 0, I(t) \geq 0, D(t) \geq 0, Q(t) \geq 0, H(t) \geq 0,$ and $R(t) \geq 0$. □

Theorem 2. *(Boundedness of the solution) The solution of the system (1) are bounded in the region* $\Omega = \left\{(S, E, I, D, Q, H, R) \in \mathbb{R}_+^7 \,\middle|\, N \leq \max\left\{N(0), \frac{\Lambda}{\mu_1}\right\}\right\}$.

Proof. Based on Theorem 1, all state variables are non-negative. From (2) an equation representing the total population is obtained as follows:

$$\frac{dN}{dT} = \Lambda - \mu_1 N,$$
$$\frac{dN}{dT} - \mu_1 N = \Lambda.$$

Using the integrating factor method through $exp\left(\int_0^t \mu_1 dt\right) = exp(\mu_1 t)$, it can be determined that $N(t)$ satisfies $N = \frac{\Lambda}{\mu_1} + N(0)exp(-\mu_h t)$. We assume the limit as $t \to \infty$, with the initial condition is higher than $\frac{\Lambda}{\mu_1}$, then the solution will continue to decrease and approach $\frac{\Lambda}{\mu_1}$. If $N(0) < \frac{\Lambda}{\mu_1}$, then the solution will continue to increase until it reaches $\frac{\Lambda}{\mu_1}$. If given $N(0) < \frac{\Lambda}{\mu_1}$, the solution remains constant at $\frac{\Lambda}{\mu_1}$. Therefore, we have $N(t) \leq \max\left\{N(0), \frac{\Lambda}{\mu_1}\right\}$. Therefore, model (1) is bounded and the theorem is proven. □

3.2 The Basic Reproduction Number of Model

In epidemiology, the basic reproductive number model ($\mathcal{R}_0$) is used to estimate how many secondary COVID-19 infections one infected person can cause in a susceptible population as the disease spreads. Furthermore, this model helps us understand the dynamics of disease transmission within a population. In addition to this, we can determine how the disease spreads in a population. The approach for determining R_0 makes use of the Next Generation Matrix (NGM), In this dynamic system model, the NGM is constructed using exposed (E) and infectious (I) individuals, we consider the following system:

$$E'(t) = \beta SE - \varepsilon E - \sigma_1 E - \mu_1 E$$
$$I'(t) = \varepsilon E - \sigma_2 I - \rho_1 I - (\mu_1 + \mu_2) I.$$

Let $Y = [E \quad I]^T$, then it can be rewritten as

$$Y' = \mathcal{F}(Y) - \mathcal{V}(Y) = \begin{bmatrix} \beta SE - \varepsilon E - \sigma_1 E - \mu_1 E \\ \varepsilon E - \sigma_2 I - \rho_1 I - (\mu_1 + \mu_2) I \end{bmatrix}.$$

The result of $\mathcal{F}(Y)$ and $\mathcal{V}(Y)$ is

$$\mathcal{F}(Y) = \begin{bmatrix} \mathcal{F}_1 \\ \mathcal{F}_2 \end{bmatrix} = \begin{bmatrix} \beta SE \\ \varepsilon E \end{bmatrix} \quad \text{and } \mathcal{V}(Y) = \begin{bmatrix} \mathcal{V}_1 \\ \mathcal{V}_2 \end{bmatrix} = \begin{bmatrix} \varepsilon E + \sigma_1 E + \mu_1 E \\ \sigma_2 I + \rho_1 I + (\mu_1 + \mu_2) I \end{bmatrix}.$$

The Jacobian matrix J is given by

$$J_{\mathcal{F}(Y)} = \begin{bmatrix} \beta S & 0 \\ \varepsilon & 0 \end{bmatrix}, \text{ then } J_{\mathcal{F}(Y_0)} = \begin{bmatrix} \beta S_0 & 0 \\ \varepsilon & 0 \end{bmatrix}.$$

Equivalently

$$J_{\mathcal{F}(Y_0)} = \begin{bmatrix} \beta \frac{\Lambda}{\mu_1} & 0 \\ \varepsilon & 0 \end{bmatrix} \text{ and } \mathcal{F} = \begin{bmatrix} \beta \frac{\Lambda}{\mu_1} & 0 \\ \varepsilon & 0 \end{bmatrix}.$$

On the other hand, we have

$$J_{\mathcal{V}(Y)} = \begin{bmatrix} \varepsilon + \sigma_1 + \mu_1 & 0 \\ 0 & \mu_1 + \mu_2 + \rho_1 + \sigma_2 \end{bmatrix} \text{ and } J_{\mathcal{V}(Y_0)} = \begin{bmatrix} \varepsilon + \sigma_1 + \mu_1 & 0 \\ 0 & \mu_1 + \mu_2 + \rho_1 + \sigma_2 \end{bmatrix}.$$

So, we have $\mathcal{V} = \begin{bmatrix} \varepsilon + \sigma_1 + \mu_1 & 0 \\ 0 & \mu_1 + \mu_2 + \rho_1 + \sigma_2 \end{bmatrix}$ then $\mathcal{V}^{-1} = \begin{bmatrix} \frac{1}{\varepsilon + \sigma_1 + \mu_1} & 0 \\ 0 & \frac{1}{(\mu_1 + \mu_2 + \rho_1 + \sigma_2)} \end{bmatrix}$.

Therefore

$$\mathcal{FV}^{-1} = \begin{bmatrix} \frac{\beta\Lambda}{\mu_1(\varepsilon+\sigma_1+\mu_1)} & 0 \\ \frac{\varepsilon}{\varepsilon+\sigma_1+\mu_1} & 0 \end{bmatrix}.$$

Reproduction number ca be defined as

$$\mathcal{R}_0 = \frac{\beta\Lambda}{\mu_1(\varepsilon+\sigma_1+\mu_1)}.$$

If $\mathcal{R}_0 < 1$, then the average infected individual transmits the infection to less than one individual during the transmission period, causing the spread rate to decrease and the infection to disappear, resulting in the epidemic stopping. If $\mathcal{R}_0 = 1$, each infected individual will produce one new infection, so the disease will remain and stabilise, but it will not cause an epidemic. On the other hand, if $\mathcal{R}_0 > 1$, each infected individual will transmit the infection to more than one new individual, causing the rate of spread to increase and potentially leading to an epidemic.

3.3 Equilibrium Points Analysis

By zeroing the right-hand side of each equation in model (1), the equilibrium points are found, as follows:

$$\begin{aligned} &\Lambda - \beta SE - \mu_1 S = 0 \\ &\beta SE - \varepsilon E - \sigma_1 E - \mu_1 E = 0 \\ &\varepsilon E - \sigma_2 I - \rho_1 I - (\mu_1 + \mu_2) I = 0 \\ &\sigma_1 E + \sigma_2 I - \rho_2 D - \mu_1 D = 0 \\ &\rho_1 I + \rho_2 D - \eta Q - (\mu_1 + \mu_2) Q = 0 \\ &\eta Q - \theta H - (\mu_1 + \mu_2) H = 0 \\ &\theta H - \mu_1 R = 0. \end{aligned} \tag{4}$$

Equation (3) can be simplified to get multiple solutions. We identify two equilibrium point states: the disease-free equilibrium point and the endemic equilibrium point. The state with no disease present is called the disease-free equilibrium. Let $\chi_0 = (S^0, E^0, I^0, D^0, Q^0, H^0, R^0) = \left(\frac{\Lambda}{\mu_1}, 0,0,0,0,0,0\right)$.

With the assistance of Maple software, we can determine the values for all variables at the endemic equilibrium points, demonstrating that these points $\chi^* = (S^*, E^*, I^*, D^*, Q^*, H^*, R^*)$, where

$$\begin{aligned} S^* &= \frac{\varepsilon+\sigma_1+\mu_1}{\beta} \\ E^* &= (\mathcal{R}_0 - 1)\frac{\mu_1}{\beta} \\ I^* &= (\mathcal{R}_0 - 1)\left(\frac{\varepsilon\mu_1}{\beta(\mu_1+\mu_2+\rho_1+\sigma_2)}\right) \\ D^* &= (\mathcal{R}_0 - 1)\left(\frac{\mu_1((\mu_1+\mu_2+\rho_1+\sigma_2)\sigma_1+\varepsilon\sigma_2)}{\beta(\mu_1+\mu_2+\rho_1+\sigma_2)(\mu_2+\rho_2)}\right) \end{aligned} \tag{5}$$

$$Q^* = (\mathcal{R}_0 - 1)\left(\frac{\mu_1\left((\mu_2\sigma_1+(\sigma_2+\rho_1+\mu_1)\sigma_1+\varepsilon(\sigma_2+\rho_1))\rho_2+\varepsilon\mu_2\rho_1\right)}{\beta(\mu_1+\mu_2+\rho_1+\sigma_2)(\mu_2+\rho_2)(\mu_2+\eta+\mu_1)}\right)$$

$$H^* = (\mathcal{R}_0 - 1)\left(\frac{(\eta-\mu_2-\mu_1)\mu_1\left((\mu_2\sigma_1+\mu_1\sigma_1+(\varepsilon+\sigma_1)(\sigma_2+\rho_1))\rho_2+\varepsilon\mu_2\rho_1\right)\mu_1}{\theta\beta(\mu_1+\mu_2+\rho_1+\sigma_2)(\mu_2+\rho_2)(\mu_2+\eta+\mu_1)}\right)$$

$$R^* = (\mathcal{R}_0 - 1)\left(\frac{(\eta-\mu_2-\mu_1)\left((\mu_2\sigma_1+(\sigma_2+\rho_1+\mu_1)\sigma_1+\varepsilon(\sigma_2+\rho_1))\rho_2+\varepsilon\mu_2\rho_1\right)}{\beta(\mu_1+\mu_2+\rho_1+\sigma_2)(\mu_2+\rho_2)(\mu_2+\eta+\mu_1)}\right).$$

IV. SENSITIVITY ANALYSIS FOR THE BASIC REPRODUCTION RATE

In this part, we conduct a sensitivity analysis with the aim of assessing the sensitivity of the basic reproduction number $\mathcal{R}_0$. to varying levels of parameter input. We employ this analysis to assess the level of change in the values of the predictor parameters that affect the dynamics of the system in question. Essential parameters must be defined in order to act as critical thresholds for illness management. The sensitivity index $\mathcal{R}_0$ is represented algebraically with regard to the parameters $\beta, \Lambda, \varepsilon, \sigma_1, \mu_1$ are as follows

1. $\mathcal{M}_\beta^{\mathcal{R}_0} = \frac{\beta}{\mathcal{R}_0}\frac{\partial \mathcal{R}_0}{\partial \beta} = 1$
2. $\mathcal{M}_\Lambda^{\mathcal{R}_0} = \frac{\Lambda}{\mathcal{R}_0}\frac{\partial \mathcal{R}_0}{\partial \Lambda} = 1$
3. $\mathcal{M}_\varepsilon^{\mathcal{R}_0} = \frac{\varepsilon}{\mathcal{R}_0}\frac{\partial \mathcal{R}_0}{\partial \varepsilon} = -\frac{\varepsilon}{\varepsilon+\mu_1+\sigma_1}$
4. $\mathcal{M}_{\sigma_1}^{\mathcal{R}_0} = \frac{\sigma_1}{\mathcal{R}_0}\frac{\partial \mathcal{R}_0}{\partial \sigma_1} = -\frac{\sigma_1}{\varepsilon+\mu_1+\sigma_1}$
5. $\mathcal{M}_{\mu_1}^{\mathcal{R}_0} = \frac{\mu_1}{\mathcal{R}_0}\frac{\partial \mathcal{R}_0}{\partial \mu_1} = -\frac{\varepsilon+2\mu_1+\sigma_1}{\varepsilon+\mu_1+\sigma_1}.$

V. BACKWARD BIFURCATION ANALYSIS

In this part, we use two theories to investigate some possible bifurcations in our system (1) center manifold theory and to construct the conditions on the parameters [31], [32]. Suppose that $\varphi = a + ib$ is a complex eigenvalue with negative real part: $i^2 = -1$, $a < 0$ and $b > 0$. We chose the transmission rate β as a bifurcation parameter, the solving $\mathcal{R}_0 = 1$, we get

$$\beta = \beta^* = \frac{\mu_1(\varepsilon + \mu_1 + \sigma_1)}{\Lambda}.$$

The Jacobian matrix $J_{(\chi_0,\beta^*)}$ for the system (1) determine at χ_0 and β^* has a simple zero eigenvalue and other eigenvalue have negative sign. Hence χ_0 is a non-hyperbolic equilibrium when $\beta = \beta^*$. Therefore, the center manifold theory can be applied. Calculating a right eigenvector $W = (w_1, w_2, w_3, w_4, w_5, w_6, w_7)$ and a left eigenvector $V = (v_1, v_2, v_3, v_4, v_5, v_6, v_7)^T$ with zero real part, we get

$$w_1 = -\frac{\Lambda\beta^*}{\mu_1(\Lambda\beta^*-\varepsilon\mu_1-\mu_1^2-\mu_1\sigma_1)}$$

$$w_2 = 1$$
$$w_3 = \frac{\varepsilon\mu_1}{(-\mu_1^2+(-\varepsilon-\sigma_1)\mu_1+\Lambda\beta^*)(\mu_1+\mu_2+\rho_1+\sigma_2)}$$
$$w_4 = -\frac{\mu_1(\mu_1\sigma_1+(\mu_2+\rho_1+\sigma_2)\sigma_1-\varepsilon\sigma_2)}{(-\mu_1^2+(-\varepsilon-\sigma_1)\mu_1+\Lambda\beta^*)(\mu_2+\rho_2)(\mu_1+\mu_2+\rho_1+\sigma_2)}$$
$$w_5 = \frac{\mu_1(-\mu_1\rho_2\sigma_1+(\varepsilon\rho_1-\rho_2\sigma_1)\mu_2+\rho_2(\varepsilon-\sigma_1)(\sigma_2+\rho_1))}{(-\mu_1^2+(-\varepsilon-\sigma_1)\mu_1+\Lambda\beta^*)(\eta+\mu_2+\rho_2)(\mu_2+\rho_2)(\mu_1+\mu_2+\rho_1+\sigma_2)}$$
$$w_6 = \frac{(\eta-\mu_1-\mu_2)\mu_1(\mu_1\rho_2\sigma_1+(-\varepsilon\rho_1+\rho_2\sigma_1)\mu_2+\rho_2(\sigma_2+\rho_1)(\sigma_1-\varepsilon))}{(-\mu_1^2+(-\varepsilon-\sigma_1)\mu_1+\Lambda\beta^*)(\eta+\mu_2+\rho_2)(\mu_2+\rho_2)(\mu_1+\mu_2+\rho_1+\sigma_2)}$$
$$w_7 = \frac{(\eta-\mu_1-\mu_2)\left((-\mu_1\sigma_1-\sigma_1\mu_2+(\varepsilon-\sigma_1)(\sigma_2+\rho_1))\rho_2+\varepsilon\mu_2\rho_1\right)}{(-\mu_1^2+(-\varepsilon-\sigma_1)\mu_1+\Lambda\beta^*)(\eta+\mu_2+\rho_2)(\mu_2+\rho_2)(\mu_1+\mu_2+\rho_1+\sigma_2)}$$

and

$$v_{1,5,6,7} = 0$$
$$v_2 = \frac{\mu_1(\mu_1\sigma_1+(\mu_2+\rho_1+\sigma_2)\sigma_1+\varepsilon\sigma_2)}{(-\mu_1^2+(-\sigma_1-\varepsilon)\mu_1+\Lambda\beta^*)(\mu_2+\rho_2)(\mu_1+\mu_2+\rho_1+\sigma_2)}$$
$$v_3 = -\frac{\sigma_2}{(\mu_2+\rho_2)(\mu_1+\mu_2+\rho_1+\sigma_2)}$$
$$v_4 = 1.$$

We calculate the bifurcation constants a and b as follows:

$$a = \sum_{n,i,j=1}^{7} v_n w_i w_j \frac{\partial^2 g_n}{\partial y_i \partial y_j}(\chi_0, \beta^*)$$
$$b = \sum_{n,i,j=1}^{7} v_n w_i \frac{\partial^2 g_n}{\partial y_i \partial \beta}(\chi_0, \beta^*)$$
$$y_1 = S, y_2 = E, y_3 = I\,, y_4 = D, y_5 = Q, y_6 = H, y_7 = R$$
$$\frac{\partial^2 g_1}{\partial y_1 \partial y_2}(\chi_0, \beta^*) = \frac{\partial^2 g_1}{\partial y_2 \partial y_4}(\chi_0, \beta^*) = -\beta^*$$
$$\frac{\partial^2 g_2}{\partial y_1 \partial y_2}(\chi_0, \beta^*) = \frac{\partial^2 g_2}{\partial y_2 \partial y_1}(\chi_0, \beta^*) = \beta^*.$$

Furthermore,

$$\frac{\partial^2 g_1}{\partial y_1 \partial \beta}(\chi_0, \beta^*) = -E$$
$$\frac{\partial^2 g_1}{\partial y_2 \partial \beta}(\chi_0, \beta^*) = -S$$
$$\frac{\partial^2 g_2}{\partial y_1 \partial \beta}(\chi_0, \beta^*) = E$$
$$\frac{\partial^2 g_2}{\partial y_2 \partial \beta}(\chi_0, \beta^*) = S$$
$$a = 2w_1w_2\left(v_1\frac{\partial^2 g_1}{\partial y_1 \partial y_2} + v_2\frac{\partial^2 g_2}{\partial y_1 \partial y_2}\right)$$
$$= 2w_1w_2(v_2\beta^* - v_1\beta^*) > 0$$
$$= -\frac{2\Lambda\beta^{*2}\mu_1(\mu_1\sigma_1 + (\mu_1+\mu_2+\rho_1+\sigma_2)\sigma_1 + \varepsilon\sigma_2)}{(-\mu_1^2 + (-\sigma_1-\varepsilon)\mu_1 + \Lambda\beta^*)(\mu_2+\rho_2)(\mu_1+\mu_2+\rho_1+\sigma_2)(\Lambda\beta^* - \varepsilon\mu_1 - \mu_1^2 - \mu_1\sigma_1)^2}$$
$$< 0$$

$$b = v_1 w_1 \frac{\partial^2 g_1}{\partial y_1 \partial \beta} + v_1 w_2 \frac{\partial^2 g_1}{\partial y_2 \partial \beta}(\chi_0, \beta^*) + v_2 w_1 \frac{\partial^2 g_2}{\partial y_1 \partial \beta}(\chi_0, \beta^*) + v_2 w_2 \frac{\partial^2 g_2}{\partial y_2 \partial \beta}(\chi_0, \beta^*)$$
$$= v_1 \left(w_1 \frac{\partial^2 g_1}{\partial y_1 \partial \beta} + w_2 \frac{\partial^2 g_1}{\partial y_2 \partial \beta} \right) + v_2 \left(w_1 \frac{\partial^2 g_2}{\partial y_1 \partial \beta} + w_2 \frac{\partial^2 g_2}{\partial y_2 \partial \beta} \right)$$
$$= v_1(-w_1 E - w_2 S) + v_2(w_1 E + w_2 S)$$
$$= \frac{\Lambda \mu_1 (\mu_1 \sigma_1 + (\mu_2 + \rho_1 + \sigma_2)\sigma_1 + \varepsilon \sigma_2)}{(\mu_2 + \rho_2)(\mu_1 + \mu_2 + \rho_1 + \sigma_2)(\Lambda \beta^* + (-\sigma_1 - \varepsilon)\mu_1 - \mu_1^2)^2} > 0.$$

It is evident that $a < 0$ and $b > 0$ when $\beta = \beta^*$.

VI. STABILITY OF THE EQUILIBRIA

6.1. Local stability analysis disease free equilibrium point

In this section, we examine the local stability of system (1) at the disease-free equilibrium point $\chi_0 = (S^0, E^0, I^0, D^0, Q^0, H^0, R^0) = \left(\frac{\Lambda}{\mu_1}, 0,0,0,0,0,0\right)$.

Theorem 3. *The disease-free equilibrium point of system (1) is locally asymptotically stable when* $\mathcal{R}_0 < 1$ *and becomes unstable when* $\mathcal{R}_0 > 1$.

Proof. The Jacobian matrix for system (1) is

$$J = \begin{bmatrix} -E\beta - \mu_1 & -S\beta & 0 & 0 & 0 & 0 & 0 \\ E\beta & S\beta - \varepsilon - \mu_1 - \sigma_1 & 0 & 0 & 0 & 0 & 0 \\ 0 & \varepsilon & -\mu_1 - \mu_2 - \rho_1 - \sigma_2 & 0 & 0 & 0 & 0 \\ 0 & \sigma_1 & \sigma_2 & -\mu_2 - \rho_2 & 0 & 0 & 0 \\ 0 & 0 & \rho_1 & \rho_2 & -\eta - \mu_1 - \mu_2 & 0 & 0 \\ 0 & 0 & 0 & 0 & \eta - \mu_1 - \mu_2 & -\theta & 0 \\ 0 & 0 & 0 & 0 & 0 & \theta & -\mu_1 \end{bmatrix}$$

which implies

$$J(\chi_0) = \begin{bmatrix} -\mu_1 & -\frac{\beta\Lambda}{\mu_1} & 0 & 0 & 0 & 0 & 0 \\ 0 & \frac{\beta\Lambda}{\mu_1} - \varepsilon - \mu_1 - \sigma_1 & 0 & 0 & 0 & 0 & 0 \\ 0 & \varepsilon & -\mu_1 - \mu_2 - \rho_1 - \sigma_2 & 0 & 0 & 0 & 0 \\ 0 & \sigma_1 & \sigma_2 & -\mu_2 - \rho_2 & 0 & 0 & 0 \\ 0 & 0 & \rho_1 & \rho_2 & -\eta - \mu_1 - \mu_2 & 0 & 0 \\ 0 & 0 & 0 & 0 & \eta - \mu_2 - \mu_2 & -\theta & 0 \\ 0 & 0 & 0 & 0 & 0 & \theta & -\mu_1 \end{bmatrix}.$$

The Jacobian matrix's characteristic polynomial at disease-free equilibrium is $det|J(\chi_0) - \lambda I| = 0$, where I is the identity matrix and λ is the eigenvalue. Thus the determinant $|J(\chi_0) - \lambda I|$ is

$$\begin{vmatrix} -\mu_1 & -\frac{\beta\Lambda}{\mu_1} & 0 & 0 & 0 & 0 & 0 \\ 0 & \frac{\beta\Lambda}{\mu_1} - \varepsilon - \mu_1 - \sigma_1 & 0 & 0 & 0 & 0 & 0 \\ 0 & \varepsilon & -\mu_1 - \mu_2 - \rho_1 - \sigma_2 & 0 & 0 & 0 & 0 \\ 0 & \sigma_1 & \sigma_2 & -\mu_2 - \rho_2 & 0 & 0 & 0 \\ 0 & 0 & \rho_1 & \rho_2 & -\eta - \mu_1 - \mu_2 & 0 & 0 \\ 0 & 0 & 0 & 0 & \eta - \mu_2 - \mu_2 & -\theta & 0 \\ 0 & 0 & 0 & 0 & 0 & \theta & -\mu_1 \end{vmatrix} = 0.$$

This results in the characteristic equation given by

$$(\lambda + \mu_1)^2(\lambda + \theta)(\lambda + \mu_2 + \rho_2)(\lambda + \mu_1 + \mu_2 + \rho_1 + \sigma_2)(\lambda + \eta + \mu_1 + \mu_2)\big(\lambda + (\mathcal{R}_0 - 1)(\varepsilon + \mu_1 + \sigma_1)\big) = 0$$

solving for λ, gives

$$\lambda_{1,2} = -\mu_1 < 0$$
$$\lambda_3 = -\theta < 0$$
$$\lambda_4 = -\mu_2 - \rho_2 < 0$$
$$\lambda_5 = -\mu_1 - \mu_2 - \rho_1 - \sigma_2 < 0$$
$$\lambda_6 = -\eta - \mu_1 - \mu_2 < 0$$
$$\lambda_7 = (\mathcal{R}_0 - 1)(\varepsilon + \mu_1 + \sigma_1) < 0$$

provided that $\mathcal{R}_0 < 1$, which complete prove and χ_0 is locally asymptotically stable. □

6.2. Local stability analysis endemic equilibrium point

The stability analysis for endemic equilibrium point is presented as follows:

Theorem 4. *The endemic equilibrium χ_1^* is locally asymptotically stable if $\mathcal{R}_0 > 1$.*

Proof. Substitution the endemic equilibrium χ_1^* in equation (A) , we get

$$J(\psi_2) = \begin{bmatrix} -\frac{(\mathcal{R}_0 - 1)\mu_1\beta\Lambda}{\beta\Lambda + \mu_1(-\varepsilon - \sigma_1) - \mu_1^2} & \varepsilon - \mu_1 - \sigma_1 & 0 & 0 & 0 & 0 & 0 \\ (\mathcal{R}_0 - 1)\mu_1 & 0 & 0 & 0 & 0 & 0 & 0 \\ 0 & \varepsilon & -\mu_1 - \mu_2 - \rho_1 - \sigma_2 & 0 & 0 & 0 & 0 \\ 0 & \sigma_1 & \sigma_2 & -\mu_2 - \rho_2 & 0 & 0 & 0 \\ 0 & 0 & \rho_1 & \rho_2 & -\eta - \mu_1 - \mu_2 & 0 & 0 \\ 0 & 0 & 0 & 0 & \eta - \mu_2 - \mu_2 & -\theta & 0 \\ 0 & 0 & 0 & 0 & 0 & \theta & -\mu_1 \end{bmatrix}$$

$$det(J(\psi_2) - \lambda^* I) = \begin{bmatrix} -\frac{(\mathcal{R}_0 - 1)\mu_1\beta\Lambda}{\beta\Lambda + \mu_1(-\varepsilon - \sigma_1) - \mu_1^2} - \lambda^* & \varepsilon - \mu_1 - \sigma_1 & 0 & 0 & 0 & 0 & 0 \\ (\mathcal{R}_0 - 1)\mu_1 - \lambda^* & -\lambda^* & 0 & 0 & 0 & 0 & 0 \\ 0 & \varepsilon & -(\mu_1 + \mu_2 + \rho_1 + \sigma_2) - \lambda^* & 0 & 0 & 0 & 0 \\ 0 & \sigma_1 & \sigma_2 & -(\mu_2 + \rho_2) - \lambda^* & 0 & 0 & 0 \\ 0 & 0 & \rho_1 & \rho_2 & -(\eta + \mu_1 + \mu_2) - \lambda^* & 0 & 0 \\ 0 & 0 & 0 & 0 & \eta - \mu_2 - \mu_2 & -\theta - \lambda^* & 0 \\ 0 & 0 & 0 & 0 & 0 & \theta & -\mu_1 - \lambda^* \end{bmatrix}.$$

Eigenvalue of λ^* of the Jacobian matrix at χ_1^* gives

$\lambda_1^* = -\mu_1 < 0$
$\lambda_2^* = -\theta < 0$

$\lambda_3^* = -\mu_2 - \rho_2 < 0$
$\lambda_4^* = -\mu_1 - \mu_2 - \rho_1 - \sigma_2 < 0$
$\lambda_5^* = -\eta - \mu_1 - \mu_2 < 0$
$\lambda_6^* = -\frac{\beta\Lambda - \sqrt{\Phi}}{2(\varepsilon + \sigma_1 + \mu_1)}$
$\lambda_7^* = -\frac{\beta\Lambda + \sqrt{\Phi}}{2(\varepsilon + \sigma_1 + \mu_1)}$
$\Phi = \Lambda\beta(\Lambda\beta - 4\varepsilon^2 - 8\varepsilon\mu_1 - 8\varepsilon\sigma_1 - 4\mu_1^2 - 8\mu_1\sigma_1 - 4\sigma_1^2)$
$+4\varepsilon\mu_1(\varepsilon^2 + 3\varepsilon\mu_1 + 3\varepsilon\sigma_1 + 3\mu_1^2 + 6\mu_1\sigma_1 + 3\sigma_1^2)$

$+4\mu_1(\mu_1^3 + 3\mu_1^2\sigma_1 + 3\mu_1\sigma_1^2 + \sigma_1^3).$

Thus, the endemic equilibrium χ_1^* demonstrates local asymptotic stability when the reproduction number exceeds 1. □

6.3. Global stability analysis

In this section, the subsequent theorems address the global stability of both the disease-free and endemic equilibrium.

Theorem 5 *The disease-free equilibrium point is globally asymptotically stable if* $\mathcal{R}_0 < 1$ *and otherwise unstable.*

Proof. The proven of the global stability of disease-free equilibrium investigate by using an approach presented by Castillo-Chavez and Song [33]. The model (1) we can write as follows:

$\frac{d\chi}{dt} = F(\chi, \mathcal{Z})$

$\frac{d\mathcal{Z}}{dt} = G(\chi, \mathcal{Z}),$ with $G(\chi, 0) = 0,$

where $\chi = (S, H, R) \in \mathbb{R}_+^3$ represents the number of disease-free components and $\mathcal{Z} = (E, I, D, Q) \in \mathbb{R}_+^4$ represents the number of disease components [34]. The following conditions (H_1) and (H_2) are required for the global asymptotic stability of the DFE of system (1) as follow:

(H_1) For $\frac{d\chi}{dt} = F(\chi, 0)$, χ_0 is globally asymptotically stable; where $F(\chi_0, 0) = 0$,

(H_2) $G(\chi, \mathcal{Z}) = A\mathcal{Z} - \hat{G}(\chi, \mathcal{Z}), \hat{G}(\chi, \mathcal{Z}) \geq 0$ for $(\chi, \mathcal{Z}) \in \Omega$, where $A = D_{\mathcal{Z}} G(\chi_0, 0)$ is a Metzler Matrix. The off diagonal elements of A are non-negative and Ω is the region where the model makes biological sense, which results in

$$\frac{d\chi}{dt} = F(\chi, \mathcal{Z}) = \begin{bmatrix} \Lambda - \beta SE - \mu_1 S \\ \eta Q - \theta H - (\mu_1 + \mu_2)H \\ \theta H - \mu_1 R \end{bmatrix}, \; F(\chi, 0) = \begin{bmatrix} \Lambda - \mu_1 S \\ 0 \\ 0 \end{bmatrix}$$

$$\frac{d\mathcal{Z}}{dt} = G(\chi, \mathcal{Z}) = \begin{bmatrix} \beta SE - \varepsilon E - \sigma_1 E - \mu_1 E \\ \varepsilon E - \sigma_2 I - \rho_1 I - (\mu_1 + \mu_2)I \\ \sigma_1 E + \sigma_2 I - \rho_2 D - \mu_1 D \\ \rho_1 I + \rho_2 D - \eta Q - (\mu_1 + \mu_2)Q \end{bmatrix}.$$

Therefore, from the model

$$A = D_Z G(\chi_0, 0)$$
$$= \begin{bmatrix} \frac{\beta\Lambda}{\mu_1} - \varepsilon - \mu_1 - \sigma_1 & 0 & 0 & 0 \\ \varepsilon & -(\mu_1 + \mu_2 + \rho_1 + \sigma_2) & 0 & 0 \\ \sigma_1 & \sigma_2 & -(\mu_2 + \rho_2) & 0 \\ 0 & \rho_1 & \rho_2 & -(\eta + \mu_1 + \mu_2) \end{bmatrix}$$

which is a Metzler Matrix. Here $\hat{G}(\chi, \mathcal{Z}) = A\mathcal{Z} - G(\chi, \mathcal{Z})$, and so

$$\hat{G}(\chi, \mathcal{Z}) = \begin{bmatrix} \hat{G}_1(\chi, \mathcal{Z}) \\ \hat{G}_2(\chi, \mathcal{Z}) \\ \hat{G}_3(\chi, \mathcal{Z}) \\ \hat{G}_4(\chi, \mathcal{Z}) \end{bmatrix} = \begin{bmatrix} \frac{\beta E(\Lambda - \mu_1 S)}{\mu_1} \\ 0 \\ 0 \\ 0 \end{bmatrix}.$$

Since $\Lambda > \mu_1 S$, inside Ω and therefore, $\hat{G}(\chi, \mathcal{Z}) \geq 0$, the two condition (H_1) and (H_2) are satisfied, then the disease-free equilibrium point of this model is globally asymptotically stable. □

Theorem 6. *Endemic equilibrium $\chi^*$is globally asymptotical stable in the region Ω , If $\mathcal{R}_0 > 1$ otherwise unstable.*

Proof. We demonstrate the above result by creating the Lyapunov function**.** Assume $(S^*, E^*, I^*, D^*, Q^*, H^*, R^*)$is an endemic equilibrium point in system (4) We define $\mathcal{L}: \{(S^*, E^*, I^*, D^*, Q^*, H^*, R^*) \in \Upsilon: S^*, E^*, I^*, D^*, Q^*, H^*, R^* > 0\} \to \mathbb{R}$ by

$$\mathcal{L}(S^*, E^*, I^*, D^*, Q^*, H^*, R^*) = \ln[(S - S^*) + (E - E^*) + (I - I^*) + (D - D^*) + (H - H^*) + (R - R^*) + 1]. \quad (6)$$

Then $\mathcal{L}$ is C^1on the interior of Υ, χ^* is the global minimum of $\mathcal{L}$ on Υ and $\mathcal{L}(S^*, E^*, I^*, D^*, Q^*, H^*, R^*) = 0$. The time derivative of $\mathcal{L}$ computed along solutions of the model in (1) as follows:

$$\bar{\mathcal{L}} = \frac{\partial \mathcal{L}}{\partial t}\frac{dS}{dt} + \frac{\partial \mathcal{L}}{\partial t}\frac{dE}{dt} + \frac{\partial \mathcal{L}}{\partial t}\frac{dI}{dt} + \frac{\partial \mathcal{L}}{\partial t}\frac{dD}{dt} + \frac{\partial \mathcal{L}}{\partial t}\frac{dQ}{dt} + \frac{\partial \mathcal{L}}{\partial t}\frac{dH}{dt} + \frac{\partial \mathcal{L}}{\partial t}\frac{dR}{dt}$$
$$= \frac{\frac{dS}{dt} + \frac{dE}{dt} + \frac{dI}{dt} + \frac{dD}{dt} + \frac{dQ}{dt} + \frac{dH}{dt} + \frac{dR}{dt}}{\left((S - S^*) + (E - E^*) + (I - I^*) + (D - D^*) + (Q - Q^*) + (H - H^*) + (R - R^*) + 1\right)}$$
$$N^* = S^* + E^* + I^* + D^* + Q^* + H^* + R^* = \frac{\Lambda}{\mu_1}.$$

Also, $N = e^{-\mu_1 t} + \frac{\Lambda}{\mu_1}$, where C is the value satisfies the condition $N(0) = \frac{\Lambda}{\mu_1}$

$$\mathcal{L} = \ln[N - N^* + 1] \geq 0$$
$$\bar{\mathcal{L}} = \frac{1}{N - \frac{\Lambda}{\mu_1} + 1}\frac{dN}{dt} = \frac{\mu_1}{N - \frac{\Lambda}{\mu_1} + 1}\left(\frac{\Lambda}{\mu_1} - N\right) \leq 0.$$

The function $\bar{\mathcal{L}}$ is negative and equals zero only when $S = S^*, E = E^*, I = I^*, D = D^*, Q = Q^*, H = H^*, R = R^*$. Thus, $\bar{\mathcal{L}}$ functions as a Lyapunov function for the system defined in model

(1). Based on the Lyapunov asymptotic stability theorem, the endemic equilibrium χ^* is globally asymptotically stable. □

VII. NUMERICAL SIMULATION RESULTS

Model simulations are conducted using parameter values sourced from various existing literature. Numerical simulation for model (1) were performed using parameter values on Table 2 obtained from various existing literature sources [13][35][36][37] [38]. This section discusses sensitivity analysis, dynamic population simulation and the effects of varying several initial value variable and parameters. Numerical simulations in this study were conducted using the Runge–Kutta fourth-order method. Given the parameter estimates in Table 2.

Table 2. Parameter Estimation

Parameter	Value	Unit	Reference
Λ	3.94	day^{-1}	[35]
β	$3.604\ 10^{-8}$	day^{-1}	[35]
μ_1	0.0999	day^{-1}	[35]
μ_2	$6.15\ 10^{-2}$	day^{-1}	[36]
ε	0.0473	day^{-1}	[36]
σ_1	0.9911	day^{-1}	[37]
σ_2	0.0758	day^{-1}	[37]
ρ_1	$2.6782\ 10^{-14}$	day^{-1}	[36]
ρ_2	0.025	day^{-1}	[38]
η	$3.72\ 10^{-2}$	day^{-1}	[13]
θ	$9.35\ \ 10^{-3}$	day^{-1}	[13]

Furthermore, to calculate the number of susceptible individuals infected, substitute the parameter values from Table 2 into the basic reproduction number.

$$\mathcal{R}_0 = \frac{\beta\Lambda}{\mu_1(\varepsilon + \sigma_1 + \mu_1)} \approx 2.0234.$$

This show indicates that each infected individual will transmit the disease to 2 other individuals. An $\mathcal{R}_0$value greater than one indicates the potential for an endemic occurrence.

7.1 Sensitivity analysis

This section presents the results of the sensitivity analysis used to identify critical parameters that have a significant impact on $\mathcal{R}_0$, with the sensitivity index of the parameters shown in the Table 3. The sensitivity index of the basic reproduction number $\mathcal{R}_0$ t to the model parameters shows that if there is an increase or decrease in the value of the parameters, it will result in a decrease or increase in $\mathcal{R}_0$. Table 2 shows the parameter values and model index. (1). The positive values of the indices Λ and β indicate the sensitivity of the reproduction number to a 10% change in the effective rate. As a result, both parameters contribute positively to the value of $\mathcal{R}_0$. Similarly, the negative sensitivity to $\mathcal{R}_0$ is measured by $\mu_1, \varepsilon,$ and σ_1, where each parameter causes a decrease in $\mathcal{R}_0$while the other parameters remain constant. For example, if

individuals apply ε of 10%, $\mathcal{R}_0$will increase by 8.7%. Figure 2 illustrates the parameters that influence COVID-19 infections, both positively and negatively.

Table 3. Indices of parameter sensitivity analysis

Parameter	Value	Sensitivity index
$\boldsymbol{\Lambda}$	3.94	1
$\boldsymbol{\beta}$	$3.604\ 10^{-8}$	1
$\boldsymbol{\mu_1}$	0.0999	-1.087
$\boldsymbol{\varepsilon}$	0.0473	-0.870
$\boldsymbol{\sigma_1}$	0.9911	-0.0415

Figure 2. Elasticity indices of parameters in determining $\mathcal{R}_0$

7.2 Dynamic population simulation

The numerical simulation of model (1) was simulated using the fourth-order Runge-Kutta method. There are seven plots representing various human populations. So, we investigated the stability of the endemic equilibrium point of model (1) where $\mathcal{R}_0 = 2.023$. To describe this endemic simulation, we used the following initial values: $S(0) = 99;\ E(0) = 90; I(0) = 63; D(t) = 35; Q(t) = 45;\ H(0) = 43; R(0) = 67$. Figure 3 shows a curve representation of the numerical solutions converging to a stable endemic equilibrium.

Figure 3 illustrates the dynamics of epidemiology by showing the changes in the number of people in various categories (Susceptible, Exposed, Infected, Quarantined, Detected, Hospitalized, and Recovered) over time (days).

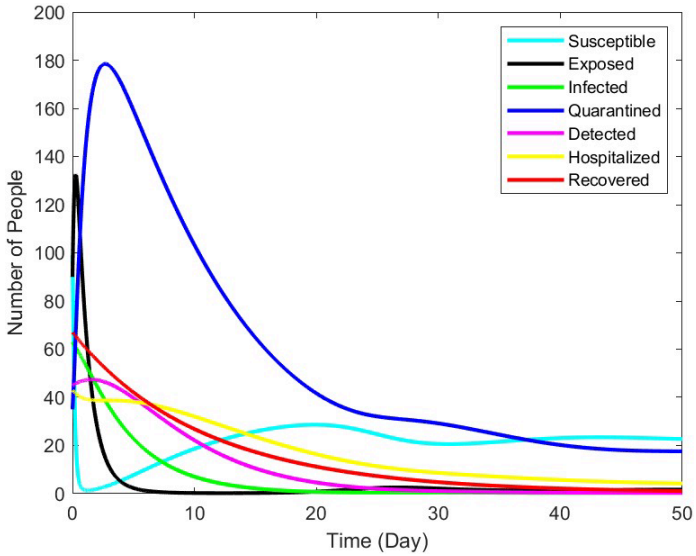

Figure 3. Numerical simulation for SEIQDHR model

The number of susceptible individuals is at its peak initially, leading to an increase in exposed and infected individuals occurring on days 1 to 5. The number of diagnosed individuals decreases on day 10, as those diagnosed will undergo quarantine. Thus, the number of individuals in quarantine increased until day 10 because several infected individuals and diagnosed individuals were undergoing quarantine. The number of individuals exposed peaks at 60 individuals. After that, it decreases, but the number of infected and quarantined individual peaks at 60 individuals and 180 individuals, respectively. The increase in the number of individuals in quarantine is attributed to the addition of individuals who were infected and detected as infected with COVID-19. The number of detected individual peaks at 45 individuals. Individuals hospitalized and recovered due to COVID-19 peak at 40 individuals and 65 individuals, respectively.

7.3 The effects of varying several parameters

In this section, the effects of parameters variations β, σ_1, and σ_2 on the number of individuals infected, quarantined, detected, and hospitalized will be simulated. Figure 4 illustrates the effect of varying the transmission rate from exposed individuals to infected (β) with values of $\beta = 0.0012; 0.056; 0.296;$ and 0.975. The simulation results show that the value of β has an impact on the number of individuals who are infected, quarantined, detected, and hospitalized. The number of infected individuals with a β value of 0.0012 as many as 6 people and with a β value of 0.975, the number of infected individuals increases to 8 people. For detected individuals, at $\beta = 0.0012$ there are 21 people, $\beta = 0.975$ the number increases to 23 people. Furthermore, for individuals hospitalized, at $\beta = 0.0012$ there are 22 people and $\beta = 0.975$ it increases to 33 people. the number of individuals in quarantine at $\beta = 0.0012$ as many as 61 and $\beta = 0.975$ as many as 119 people. Consequently, the increase in the transmission rate of exposed individuals becoming infectious from 0.0012 to 0.975 leads to an increase in the number of infected, quarantined, detected, and hospitalized individuals.

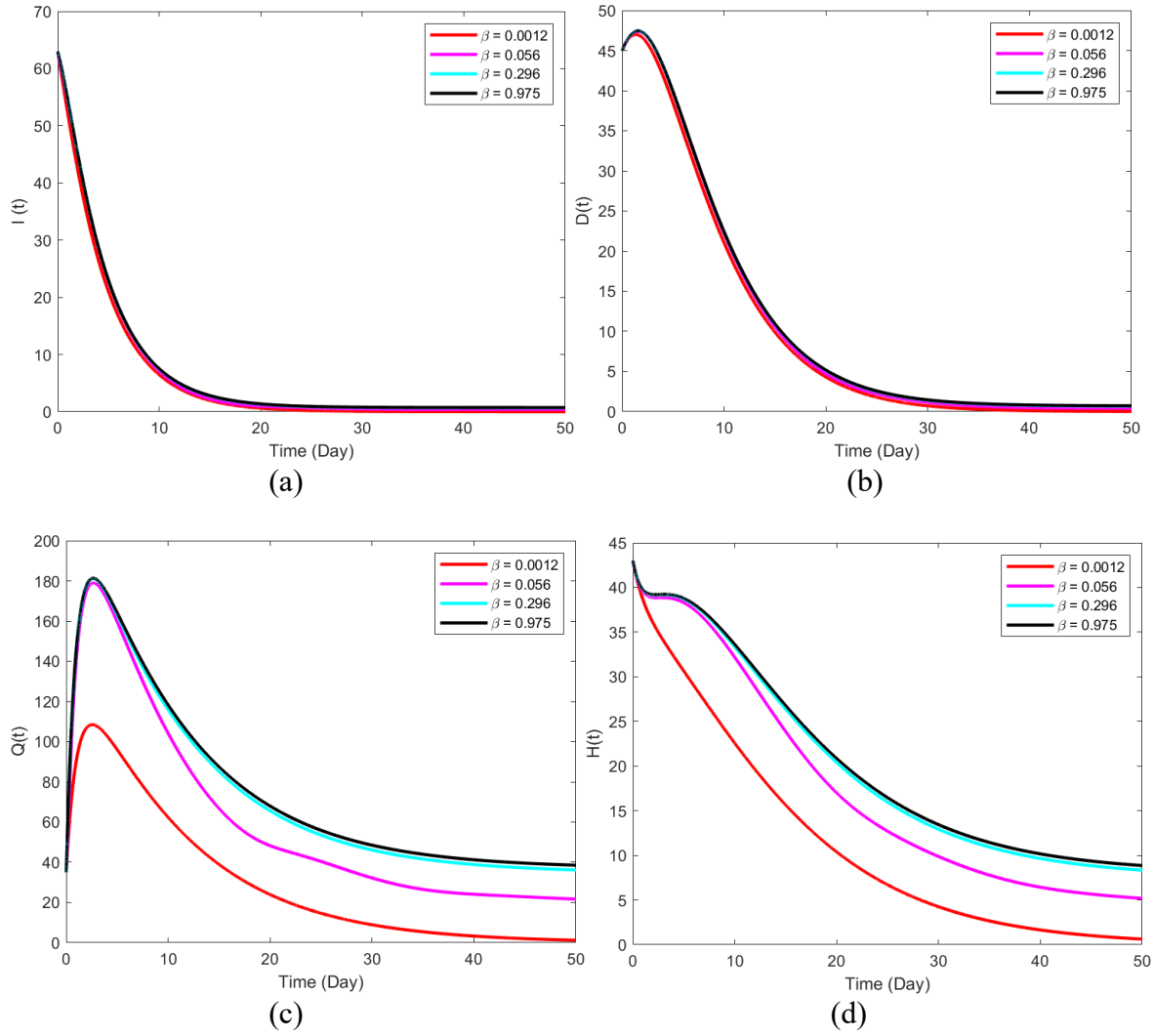

Figure 4. Effect of β on $I(t)$, $D(t)$, $Q(t)$, $H(t)$

Figure 5 shows the detection rate of exposed individuals (σ_1) on the 10th day with variations in parameter values are 0.0037, 0.016, 0.351, and 0.995. The results obtained indicate that the increase in the value of $\sigma_1$significantly affects the reduction of infected individual and detected individuals. On the other hand, quarantined individual and hospitalize individual has increased. The simulation shows that individuals infected with a value of $\sigma_1 = 0.995$ as many as 6 people, while those with a value of $\sigma_1 = 0.0037$ as many as 32 people. For individuals detected with $\sigma_1 = 0.995$ as many as 23 people, whereas with $\sigma_1 = 0.0037$, the number increases as many as 40 people. Individuals in quarantine, with $\sigma_1 = 0.995$ as many as 102 people, whereas $\sigma_1 = 0.0037$ as many as 36 people. Next, the number of individuals receiving treatment is also shown, where the value $\sigma_1 = 0.995$ as many as 31 people, while at $\sigma_1 = 0.0037$ as many as 14 people.

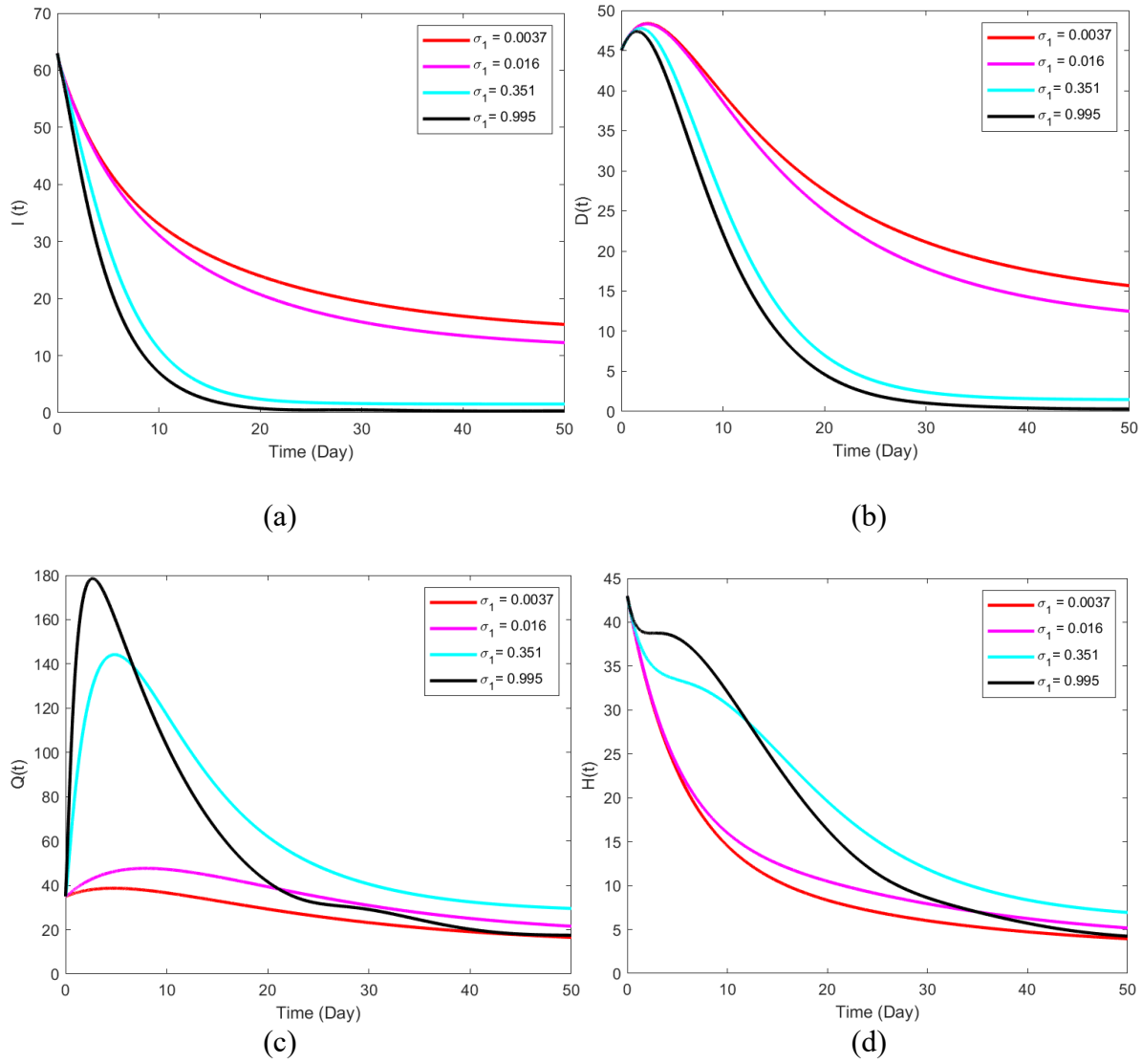

Figure 5. Effect of σ_1 on $I(t)$, $D(t)$, $Q(t)$, $H(t)$

Figure 6 illustrates the detection rate of infected individuals (σ2), with values $\sigma_2 = 0.0054$; $\sigma_2 = 0.013$; $\sigma_2 = 0.05$; and $\sigma_2 = 0.202$. The simulation shows that the number of infected individuals with a value of $\sigma_2 = 0.0054$ as many as 13 people and $\sigma_2 = 0.202$ as many as 2 people. Next, the number of individuals detected with a value of $\sigma_2 = 0.0054$ as many as 36 people, and with $\sigma_2 = 0.202$ as many as 9 people. This indicates that the rate of detecting infected individuals can reduce the number of infected and detected individuals. However, the detection rate of infected individuals at $\sigma_2 = 0.202$can increase the quarantined individuals and hospitalize individuals as many as 110 people and 34 people respectively.

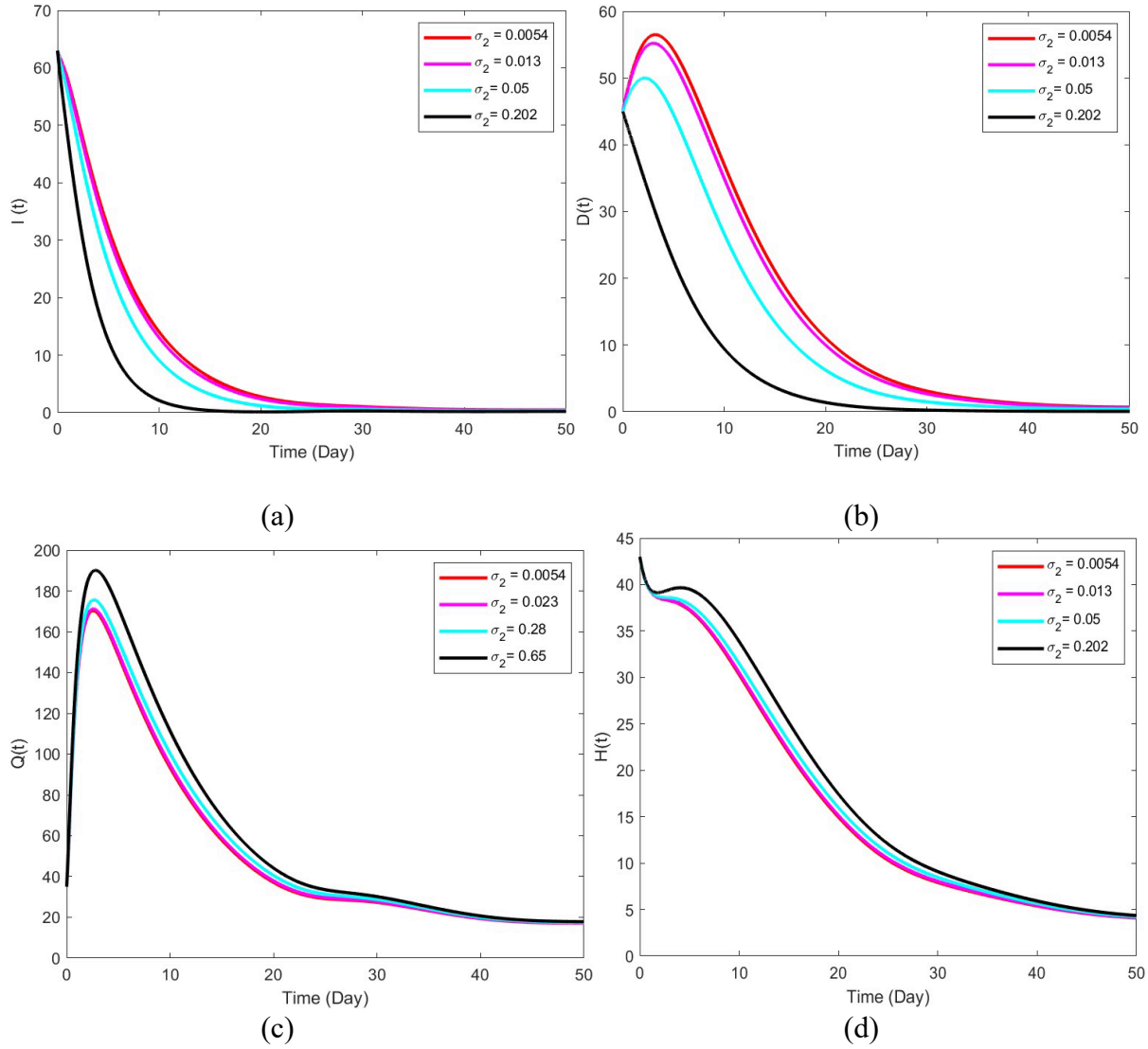

Figure 6. Effect of σ_2 on $I(t)$, $D(t)$, $Q(t)$, $H(t)$

VIII. CONCLUSION

In this paper, we develop and analyze the deterministic ODE model SEIQDHR (Susceptible - Exposed - Infected - Quarantined - Detected or Diagnosed - Hospitalized - Recovered) to study the impact of various interventions on the spread of COVID-19. The basic reproduction number associated with this model is obtained using the Next Generation Matrix. We investigate the disease-free and endemic equilibrium points, and analyze their local stability using the Routh-Hurwitz criterion. Additionally, a global stability analysis was conducted at the disease-free equilibrium point using the Metzler Matrix and at the endemic equilibrium point using the Lyapunov function. Based on the sensitivity analysis, the parameters that influence the dynamics of disease spread in the model are the transmission rate of exposed individuals getting infectious, the progression rate from exposed individuals to infectious individuals, and the rate for the detection of exposed individuals. To validate the developed

model, we conducted numerical simulations on the model. The implementation of early detection and individual hospitalization is carried out effectively on susceptible, exposed, and infected populations to reduce disease transmission.

In addition, numerical simulations were conducted to validate the proposed model. Various scenarios were tested using different parameter values related to detection. The established parameters indicate that increasing early detection steps for individual identification has proven effective, especially in infected populations. This indicates that detection interventions can help reduce the spread of COVID-19. Thus, this research is expected to support stakeholders and health professionals in maximizing these intervention mechanisms to reduce the spread of COVID-19 in the future.

The proposed research model is preliminary, and potential researchers can develop it in various ways, such as by incorporating additional compartments, optimal control approaches, and fractal-fractional order.

REFERENCES

[1] A. S. Mata and S. M. P. Dourado, "Mathematical modeling applied to epidemics: an overview," *São Paulo Journal of Mathematical Sciences*, vol. 15, no. 2, pp. 1025–1044, Dec. 2021, doi: 10.1007/s40863-021-00268-7.

[2] Y. Guo *et al.*, "Impact of public health and social measures on contact dynamics during a SARS-CoV-2 Omicron variant outbreak in Quanzhou, China, March to April 2022," *International Journal of Infectious Diseases*, vol. 131, pp. 46–49, Jun. 2023, doi: 10.1016/j.ijid.2023.03.025.

[3] T. S. Chillon, K. Demircan, G. Weiss, W. B. Minich, M. Schenk, and L. Schomburg, "Detection of antibodies to SARS-CoV-2 after vaccination in seminal plasma and their association to sperm parameters," *International Journal of Infectious Diseases*, vol. 130, pp. 161–165, May 2023, doi: 10.1016/j.ijid.2023.03.018.

[4] H. Oumarou Hama, T. Chenal, O. Pible, G. Miotello, J. Armengaud, and M. Drancourt, "An ancient coronavirus from individuals in France, circa 16th century," *International Journal of Infectious Diseases*, vol. 131, pp. 7–12, Jun. 2023, doi: 10.1016/j.ijid.2023.03.019.

[5] S. Zannoli *et al.*, "SARS-CoV-2 coinfection in immunocompromised host leads to the generation of recombinant strain," *International Journal of Infectious Diseases*, vol. 131, pp. 65–70, Jun. 2023, doi: 10.1016/j.ijid.2023.03.014.

[6] C. Yang and J. Wang, "Transmission rates and environmental reservoirs for COVID-19 – a modeling study," *J Biol Dyn*, vol. 15, no. 1, pp. 86–108, Jan. 2021, doi: 10.1080/17513758.2020.1869844.

[7] V. Trivedi, K. K. Pandey, and A. Trivedi, "Application-Based Cab Services in India: Commuters' Barriers due to COVID-19," *International Journal of Mathematical, Engineering and Management Sciences*, vol. 7, no. 3, pp. 417–432, May 2022, doi: 10.33889/IJMEMS.2022.7.3.028.

[8] R. Kumari, N. Gupta, and N. Kumar, "Segmentation of Covid-19 Affected X-Ray Image using K-means and DPSO Algorithm," *International Journal of Mathematical, Engineering and Management Sciences*, vol. 6, no. 5, pp. 1255–1275, Oct. 2021, doi: 10.33889/IJMEMS.2021.6.5.076.

[9] P. K. Sethy, S. K. Behera, P. K. Ratha, and P. Biswas, "Detection of coronavirus Disease (COVID-19) based on Deep Features and Support Vector Machine," *International*

Journal of Mathematical, Engineering and Management Sciences, vol. 5, no. 4, pp. 643–651, Aug. 2020, doi: 10.33889/IJMEMS.2020.5.4.052.

[10] W. S. Avusuglo, N. Bragazzi, A. Asgary, J. Orbinski, J. Wu, and J. D. Kong, "Leveraging an epidemic–economic mathematical model to assess human responses to COVID-19 policies and disease progression," *Sci Rep*, vol. 13, no. 1, p. 12842, Aug. 2023, doi: 10.1038/s41598-023-39723-0.

[11] K. Das, A. Annand, and M. Ram, "A Global Supply Network Design Model: A Resilient Management Approach," *International Journal of Mathematical, Engineering and Management Sciences*, vol. 6, no. 2, pp. 660–676, Apr. 2021, doi: 10.33889/IJMEMS.2021.6.2.041.

[12] R. Cassidy *et al.*, "Mathematical modelling for health systems research: a systematic review of system dynamics and agent-based models," *BMC Health Serv Res*, vol. 19, no. 1, p. 845, Dec. 2019, doi: 10.1186/s12913-019-4627-7.

[13] Y. Liu, R. Wu, and A. Yang, "Research on Medical Problems Based on Mathematical Models," *Mathematics*, vol. 11, no. 13, p. 2842, Jun. 2023, doi: 10.3390/math11132842.

[14] A. El Bhih, Y. Benfatah, H. Hassouni, O. Balatif, and M. Rachik, "Mathematical modeling, sensitivity analysis, and optimal control of students awareness in mathematics education," *Partial Differential Equations in Applied Mathematics*, vol. 11, p. 100795, Sep. 2024, doi: 10.1016/j.padiff.2024.100795.

[15] L. D. Fernandes, A. S. Mata, W. A. C. Godoy, and C. Reigada, "Refuge distributions and landscape connectivity affect host-parasitoid dynamics: Motivations for biological control in agroecosystems," *PLoS One*, vol. 17, no. 4, p. e0267037, Apr. 2022, doi: 10.1371/journal.pone.0267037.

[16] D. Herrera, S. Tosetti, and R. Carelli, "Dynamic Modeling and Identification of an Agriculture Autonomous Vehicle," *IEEE Latin America Transactions*, vol. 14, no. 6, pp. 2631–2637, 2016, doi: 10.1109/TLA.2016.7555230.

[17] M. Pawnuk and I. Sówka, "Application of mathematical modelling in evaluation of odour nuisance from selected waste management plant," *E3S Web of Conferences*, vol. 100, p. 00063, Jun. 2019, doi: 10.1051/e3sconf/201910000063.

[18] Widowati, S. P. Putro, and E. Triyana, "Construction of lyapunov function using gradient method to stability analysis of the nitrogen-phosphate-phytoplankton-sediment interaction model," *J Phys Conf Ser*, vol. 1524, no. 1, p. 012033, Apr. 2020, doi: 10.1088/1742-6596/1524/1/012033.

[19] E. Triyana, Widowati, and S. P. Putro, "Locally stability analysis of the Phytoplankton-Nitrogen- Phosphate-Sediment dynamical system: A study case at Karimunjawa aquaculture system, Central Java," *J Phys Conf Ser*, vol. 1397, no. 1, p. 012066, Dec. 2019, doi: 10.1088/1742-6596/1397/1/012066.

[20] Y. Ucakan, S. Gulen, and K. Koklu, "Analysing of Tuberculosis in Turkey through SIR, SEIR and BSEIR Mathematical Models," *Math Comput Model Dyn Syst*, vol. 27, no. 1, pp. 179–202, Jan. 2021, doi: 10.1080/13873954.2021.1881560.

[21] A. S. Alsheri, A. A. Alraeza, and M. R. Afia, "Mathematical modeling of the effect of quarantine rate on controlling the infection of COVID19 in the population of Saudi Arabia," *Alexandria Engineering Journal*, vol. 61, no. 9, pp. 6843–6850, Sep. 2022, doi: 10.1016/j.aej.2021.12.033.

[22] R. ud Din and E. A. Algehyne, "Mathematical analysis of COVID-19 by using SIR model with convex incidence rate," *Results Phys*, vol. 23, p. 103970, Apr. 2021, doi: 10.1016/j.rinp.2021.103970.

[23] P. J. Harris and B. E. J. Bodmann, "A mathematical model for simulating the spread of a disease through a country divided into geographical regions with different population densities," *J Math Biol*, vol. 85, no. 4, p. 32, Oct. 2022, doi: 10.1007/s00285-022-01803-6.

[24] H. A. Adekola, I. A. Adekunle, H. O. Egberongbe, S. A. Onitilo, and I. N. Abdullahi, "Mathematical modeling for infectious viral disease: The COVID-19 perspective," *J Public Aff*, Aug. 2020, doi: 10.1002/pa.2306.

[25] A. S. Mata and S. M. P. Dourado, "Mathematical modeling applied to epidemics: an overview," *São Paulo Journal of Mathematical Sciences*, vol. 15, no. 2, pp. 1025–1044, Dec. 2021, doi: 10.1007/s40863-021-00268-7.

[26] K. Das, B. S. N. Murthy, Sk. A. Samad, and Md. H. A. Biswas, "Mathematical transmission analysis of SEIR tuberculosis disease model," *Sensors International*, vol. 2, p. 100120, 2021, doi: 10.1016/j.sintl.2021.100120.

[27] A. A. Thirthar, H. Abboubakar, A. Khan, and T. Abdeljawad, "Mathematical modeling of the COVID-19 epidemic with fear impact," *AIMS Mathematics*, vol. 8, no. 3, pp. 6447–6465, 2023, doi: 10.3934/math.2023326.

[28] J. M. Jonnalagadda, "Epidemic Analysis and Mathematical Modelling of H1N1 (A) with Vaccination," *Nonautonomous Dynamical Systems*, vol. 9, no. 1, pp. 1–10, Jan. 2022, doi: 10.1515/msds-2020-0143.

[29] I. U. Haq, N. Ullah, N. Ali, and K. S. Nisar, "A New Mathematical Model of COVID-19 with Quarantine and Vaccination," *Mathematics*, vol. 11, no. 1, p. 142, Dec. 2022, doi: 10.3390/math11010142.

[30] A. M. Mishra, S. D. Purohit, K. M. Owolabi, and Y. D. Sharma, "A nonlinear epidemiological model considering asymptotic and quarantine classes for SARS CoV-2 virus," *Chaos Solitons Fractals*, vol. 138, p. 109953, Sep. 2020, doi: 10.1016/j.chaos.2020.109953.

[31] Z. S. Kifle and L. L. Obsu, "Mathematical modeling for COVID-19 transmission dynamics: A case study in Ethiopia," *Results Phys*, vol. 34, p. 105191, Mar. 2022, doi: 10.1016/j.rinp.2022.105191.

[32] H. van der Veen, K. Vuik, and R. de Borst, "Branch switching techniques for bifurcation in soil deformation," *Comput Methods Appl Mech Eng*, vol. 190, no. 5–7, pp. 707–719, Nov. 2000, doi: 10.1016/S0045-7825(99)00439-9.

[33] C. Castillo-Chavez and B. Song, "Dynamical Models of Tuberculosis and Their Applications," *Mathematical Biosciences and Engineering*, vol. 1, no. 2, pp. 361–404, 2004, doi: 10.3934/mbe.2004.1.361.

[34] K. G. Mekonen, T. G. Habtemicheal, and S. F. Balcha, "Modeling the effect of contaminated objects for the transmission dynamics of COVID-19 pandemic with self protection behavior changes," *Results in Applied Mathematics*, vol. 9, p. 100134, Feb. 2021, doi: 10.1016/j.rinam.2020.100134.

[35] Widowati, Kartono, Sutrisno, R. H. S. Utomo, and E. Triyana, "Stability Analysis and Numerical Simulation of the Transmission Dynamics of Covid-19 Infection," *Migration Letters*, vol. 21, no. 4, pp. 1264–1263, Feb. 2024, [Online]. Available: https://migrationletters.com/index.php/ml/article/view/8032

[36] Widowati, Sutrisno, P. S. Sasongko, M. Brilliant, and E. Triyana, "Mathematical Modeling and Stability Analysis of the COVID-19 Spread by Considering Quarantine and Hospitalize," *Mathematical Modelling of Engineering Problems*, vol. 9, no. 6, pp. 1545–1556, Dec. 2022, doi: 10.18280/mmep.090614.

[37] M. Aakash, C. Gunasundari, S. Athithan, N. B. Sharmila, G. S. Kumar, and R. Guefaifia, "Mathematical modeling of COVID-19 with the effects of quarantine and detection," *Partial Differential Equations in Applied Mathematics*, vol. 9, p. 100609, Mar. 2024, doi: 10.1016/j.padiff.2023.100609.

[38] A. Olivares and E. Staffetti, "Optimal Control Applied to Vaccination and Testing Policies for COVID-19," *Mathematics*, vol. 9, no. 23, p. 3100, Dec. 2021, doi: 10.3390/math9233100.